Proceedings of the 71st International Astronautical Congress - the Cyberspace Edition, 10-12 October 2020, Online
https://www.iafastro.org/assets/files/publications/iac-publications/
iac2020_virtual_finalprogramme_2020-10-14_final_online_low-res.pdf

# Modified Tisserand Map Exploration for Preliminary Multiple Gravity Assist Trajectory Design

**Andrea Bellome[a]*, Joan-Pau Sanchez Cuartielles[a]*, Leonard Felicetti[a]*, Stephen Kemble[a]***

[a] *School of Aerospace Transport and Manufacturing, Cranfield University, College Road, Wharley End, Bedford, MK40 1EA, United Kingdom*
* Corresponding Author, andrea.bellome@cranfield.ac.uk, jp.sanchez@cranfield.ac.uk, leonard.felicetti@cranfield.ac.uk, stephen.kemble@cranfield.ac.uk

**Abstract**

Multiple-gravity assist (MGA) trajectories are used in interplanetary missions to change the spacecraft orbital energy by exploiting the gravity of celestial bodies. This allows the spacecraft to reach regions in the Solar System that otherwise would be extremely demanding in terms of propellant. However, if a trajectory seeks to benefit from a long MGA sequence, it is necessary to solve a complex mixed integer programming problem in order to find the best swing-by sequence among all combinations of encountered planets and dates for the various spacecraft manoeuvres.

Tisserand graphs provide an efficient way to tackle the combinatorial part of the MGA problem, by allowing a simple computation of the effect of different sequences of gravity assists, based only on energy considerations. Typically, the exploration of Tisserand graphs is performed via a comprehensive Tree Search of possible sequences that reach a specific orbital energy and eccentricity (e.g. Langouski et al.). However, this approach is generally directed by heuristic techniques aimed at finding duration limited, low $\Delta v$ transfers without formal optimization or time constraint. This results in not having information from Tisserand graphs associated to the trajectory shape, namely the planetary phasing and mission durations.

This paper presents a more comprehensive strategy involving the solution of the phasing problem to automatically generate viable ballistic planetary sequences. This approach has proven to be effective in representing trajectory shape already from the Tisserand map exploration step. All the solutions identified by the modified Tisserand map exploration are validated by re-optimizing the complete MGA trajectories as sequences of swing-bys, DSMs and Lambert Arc transfers intersecting the real positions of the planets involved. Different mission scenarios towards Jupiter are used as test cases to validate and demonstrate the accuracy of the Tisserand-based first-guess solutions.

**Keywords:** Multiple Gravity Assist, Tisserand map, Mixed-Integer optimization

## 1. Introduction

Multiple Gravity Assist (MGA) trajectories exploit successive close passages, also called flybys or swing-bys, with celestial bodies to change the spacecraft orbital energy in its interplanetary journey around the Sun. This is equivalent to gain a $\Delta$v with no propellant expenditure, thus allowing to explore regions in the solar system that would be extremely demanding to reach otherwise. For example, Galileo [1], Cassini [2] and the more recent Parker Solar Probe [3] and Solar Orbiter [4] required multiple flybys with Venus, Earth and even Jupiter to reach the desired scientific orbit.

The design of such missions presents the complication that the trajectory structure, namely the planetary sequence, is not known a priori, but is the objective of the optimization itself, leading to a complex mixed-integer non-linear programming (MINLP) problem [5], also known in literature as Hybrid Optimal Control Problem (HOCP) [6]. This is one of the most difficult types of optimization problems, as it requires the solution of a combinatorial problem mixed with optimal control theory. MINLP/HOCP can be seen as two coupled optimization problems: the combinatorial part aiming at choosing the optimal sequence of flybys, and the continuous part aiming at identifying one or more locally optimal trajectories for a candidate planetary sequence. The complexity is due to the fact that these two components are highly coupled, that is the goodness of candidate sequence depends upon the solution of the continuous optimization and a variation of even a single flyby body corresponds to a significantly different set of trajectories.

To autonomously solve an MGA problem, different strategies exist. Chilan and Conway [7], Wall and Conway [8] and Englander, Conway and Williams [9], [10] employed integer genetic algorithm and a real-valued heuristic algorithm for the combinatorial and continuous part, respectively, with both impulsive and low-thrust manoeuvres. Ceriotti and Vasile [11], [12] used a method inspired by Ant Colony Optimization (ACO) to solve the MGA problem with Deep Space Manoeuvres (DSMs). Gad and Abdelkhalik [13], [14] applied a real-valued genetic algorithm using ‘hidden



Copyright © 2019 The Authors. This is the Author Original Manuscript. Permission for reuse should be obtained from the corresponding author.

genes' and dynamic population size to find flyby sequences and the associated optimal trajectory. Schlueter et al. [5] formulated the MGA trajectory design as a MINLP problem, and used a combination of ACO and Sequential Quadratic Programming (SQP) to simultaneously solve the combinatorial and continuous problem, provided a fixed length of the planetary sequence.

Strange and Longuski [15] developed a graphical technique based on Tisserand criterion to look for ballistic flyby tours to a given destination. Tisserand graphs provide an efficient way to tackle the combinatorial part of the MGA problem, by allowing a simple computation of the effect of different sequences of gravity assists, based only on energy considerations, not considering planetary phasing. They have been applied in many complex MGA trajectory designs. For example, Kloster et al. [16] and Colasurdo et al. [17] used Tisserand graphs to assess the feasibility of moon tours around Jupiter while Chen et al. [18] and Sun et al. [19] studied the accessibility of main-belt and near-Earth asteroids via MGA transfers derived from Tisserand graph exploration. However, even though Tisserand graphs can quickly assess the feasibility of different gravity assist sequences, there is no explicit information about mission duration or eventual DSM. In this way, the combinatorial solution only provides sequences which are energetically possible, but planets synchronicity might never occur.

In this paper, we present a novel strategy inspired by Tisserand graphs which allows for more truthful representation of MGA transfers. Extra realism in the mission duration evaluation is achieved by considering planetary phasing as well as resonances when stepping along an infinity velocity contour, to ensure feasible transfer durations, while maintaining limited the run time. In particular, Section 2 classifies MGA trajectory design as a MINLP problem, Section 3 introduces Tisserand maps and provides details on how to employ them to construct planetary sequences. Section 4 shows the continuous MGA trajectory optimization, aiming at finding at least one locally optimal trajectory for a given sequence. Section 5 introduces the modified Tisserand map exploration with the solution of the phasing problem, while Section 6 provides details on results obtained with the proposed solution.

## 2. Multiple Gravity Assist Trajectory Design

The MGA trajectory design is a global optimization problem in its nature, as for a given trajectory option, namely a planetary sequence, there exist several locally optimal trajectories, in terms of planets phasing, presence of DSMs, etc. Designing an MGA trajectory corresponds to solve a MINLP problem, as it involves the optimization of both integer and continuous variables. A general formulation of a MINLP is provided as follows [5], where f(x,y) is the objective function to be minimized:

Minimize:

$$f(x,y),(x \in R^{n_{cont}}, y \in Z^{n_{int}}, n_{cont}, n_{int} \in N)$$

Subject to:

$$g_i(x,y) = 0, \quad i = 1,\dots,m_e \in N$$
$$g_j(x,y) \geq 0, \quad j = 1,\dots,m_i \in N$$
$$x_l \leq x \leq x_u, \quad (x_l, x_u \in R^{n_{cont}})$$
$$y_l \leq y \leq y_l, \quad (y_l, y_u \in R^{n_{cont}})$$

Table 1. (x,y) components employed in full MGA trajectory design

| Discrete variables | Description | Continuous variables | Description |
|---|---|---|---|
| $y_1$ | Departing planet (e.g. the Earth) | $t_0$ (MJD2000) | Departing date |
| | | $v_{\infty D}$ (km/s) | Departing infinity velocity |
| | | $\alpha_{\infty D}$ (deg) | Departing angle |
| $y_i$, i=2,…, $n_{int}$-1 | Swing-by planets (e.g. Venus, Earth, Mars) | $TOF_i$ (days) | Time of flight to planet i |
| | | $\alpha_i$ | Fraction of $TOF_i$ at which a DSM occurs |
| | | $\gamma_i$ (deg) | Inclination of the flyby plane at planet i |
| | | $h_i$ (km) | Flyby periapsis altitude at planet i |
| $y_{n,int}$ | Arrival planet (e.g. Jupiter) | $TOF_{n,int}$ (days) | Time of flight towards planet $n_{int}$ |
| | | $\alpha_{int}$ | Fraction of $TOF_{n,int}$ at which a DSM occurs |

Vectors $(x, y)$ include the decision variables of the optimization: the components of $x$ are the continuous variables, while the components of vector $y$ are the discrete variables. Moreover, the decision variables $(x, y)$ are constrained by lower $(x_l, y_l)$ and upper bounds $(x_u, y_u)$. $g_i(x,y) = 0$ and $g_j(x,y)$ represents the equality and inequality constraints, respectively, which the optimization is subject to; $n_{cont}$ and $n_{int}$ are the cardinality of $x$ and $y$, respectively; $m_e$ and $m_i$ are the cardinality of the equality and inequality constraints, respectively.. In an MGA mission design, the discrete

components of $y$ correspond to the unknown planetary sequence, while x includes the continuous-varying variables as the launch date and four variables for each of the gravity-assist planets, that are the time of flight between two successive planetary encounters, flyby altitudes, hyperbola plane inclination and presence of DSM. The combination of discrete and continuous variables forms a challenging MINLP problem, as a variation of even a single component of $y$ vector corresponds to a considerably different x vector. Table 1 summarises all (x,y) components usually employed for MGA trajectory design. Due to high complexity of global optimization [20], MGA trajectory design was used to challenge the space community with the 'nearly impossible' Global Trajectory Optimization Completions (GTOCs), as in Izzo [21], where a complex MGA transfer was to be designed to reach and impact a potentially hazardous asteroid.

In this paper, the design of an interplanetary mission from Earth to Jupiter is analysed. This is a very well-known MGA transfer problem as it is based on NASA mission Galileo (see D'Amario et al. [1] or Meltzer [22]), as well as on ESA 2022 JUICE mission (see Grasset et al. [23] or Ecale et al. [24]), and it is usually used in literature for benchmarking, such as in Petropoulos et al. [25], Schlueter et al. [5] or Olds et al. [26]. This has proven to be a quite complex problem, as designing trajectories to high heliocentric orbital energies usually requires complex MGA transfers, on which the spacecraft increases its energy with low propellant consumption. The Galileo mission exploited three flybys, one at Venus and two at Earth, to reach Jupiter, while JUICE is intended to perform several swing-bys at Earth, Venus and Mars to achieve the desired energy.

The model employed in the present work is based on the patched-conics approximation as described by Vallado [27], on which the interplanetary legs, i.e. the trajectories between two successive planetary encounters, are assumed to be Keplerian, with the Sun as the main attracting body and the planets gravity influence is neglected. In this present paper, these planet-to-planet trajectories are defined as two ballistic arcs interconnected by a deep-space manoeuvre. This thus represent that the trajectories are solved by defining the direction and magnitude of the departure velocity from the departure planet, the time span until the second planet and the date of encounter with the arrival planet. The second ballistic arc is solved as a Lambert arc solutions [28].

A flyby is then assumed any time the spacecraft position with respect to the Sun matches the one of the planets. The planetary gravitational influence is assumed to affect the spacecraft motion only inside the planet Sphere of Influence (SOI), but the latter is assumed of negligible size as compared with the Solar System. The flyby model used here is the one described in Vallado [27]. In this way, a flyby corresponds to an instantaneous change of the spacecraft heliocentric velocity, (see Fig. 1) depending upon the spacecraft velocity with respect to the planet (i.e. $V_\infty$) and the deflection (i.e. $\delta$), which eventually is linked to the flyby periapsis (i.e. $r_p$) by:

$$\sin\left(\frac{\delta}{2}\right) = \left(1 + \frac{r_p V_\infty^2}{\mu_{PL}}\right)^{-1} \tag{1}$$

Where $\mu_{PL}$ is s the gravitational parameter of the swing-by planet.

In order to assess the feasibility of different trajectory options, Tisserand graphs [15] are employed to generate the gravity-assist bodies. These allow for fast computation of the effect of a flyby with a given planet, only employing energetic considerations. In this way, it is possible to tackle the combinatorial part of the MGA-MINLP optimization problem, by analysing different planetary sequences. The next section provides details of Tisserand graphs as used in the present work.

## 3. Tisserand Graphs

Tisserand graph is a graphical technique first introduced in Strange and Longuski [15] which can be used in interplanetary mission design for quick computation of sequences of gravity-assist bodies. Tisserand graphs can be obtained by parametrizing the Tisserand invariant [29] with respect to the infinity velocity of the spacecraft relative to the gravity assist body [30].

It is thus possible to visualise how a gravity assist changes the orbit of the spacecraft relating the Tisserand invariant and the turning angle $\alpha$ (see Fig. 1) with the resulting orbit of the spacecraft as done in [31]:

$$\begin{cases} \frac{R_{PL}}{a_{SC}} = 2 - \frac{1}{V_{PL}^2}\left(V_\infty^2 + V_{PL}^2 + 2V_\infty V_{PL}\cos\alpha\right) \\ e_{SC}^2 = 1 - \frac{1}{4}\frac{R_{PL}}{a_{SC}}\left(3 - \left(\frac{V_\infty}{V_{PL}}\right)^2 - \frac{R_{PL}}{a}\right)^2 \end{cases} \tag{2}$$

Where $R_{PL}$ and $V_{PL}$ are the distance and velocity magnitudes of the flyby planet with respect to the Sun, respectively, $a_{SC}$ and $e_{SC}$ are the semi-major axis and eccentricity of the spacecraft orbit, respectively, $V_\infty$ is the infinity velocity magnitude of the spacecraft with respect to the flyby planet and $\alpha$ is the flight path angle, ranging from $0^o$ to $180^o$. The term $3 - (V_\infty/V_{PL})^2$ represents the Tisserand invariant, assuming the planets orbits be circular and coplanar, which is an acceptable assumption in preliminary mission design. All the planets obits are inclined only by few degrees with respect to the ecliptic plane (Venus and Mercury have

the highest inclination of $3.4\,deg$ and $7\,deg$, respectively); moreover, only Mercury and Mars have the most eccentric orbits ( $0.20563$ and $0.09340$, respectively), while the other planets have nearly circular paths [27].

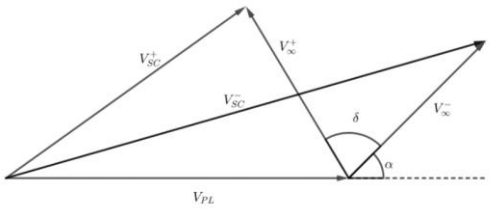


Fig. 1. Vector diagram representing the effect of a flyby with a generic planet

The vector diagram in Fig. 1 represents the effect of a close passage with a generic planet with velocity $V_{PL}$. The velocity of the spacecraft before the flyby is $V_{SC}^{-}$, while the velocity after the flyby is $V_{SC}^{+}$. The turning angle $\delta$ determines the orbit of the spacecraft after the flyby, rotating the infinity velocity vector from $V_{\infty}^{-}$ to $V_{\infty}^{+}$. The flyby can be assumed to occur instantaneously when compared to the interplanetary travel times. From Fig. 1, if $\alpha$ is equal to zero, then the spacecraft velocity is aligned with the planet one, corresponding to the highest orbital energy for a given $V_{\infty}$ magnitude (see also Fig. 2). If $\alpha$ is equal to $180^{o}$, the velocity of the spacecraft is antiparallel to the planet's one, resulting in the lowest orbital energy for the given $V_{\infty}$ magnitude.

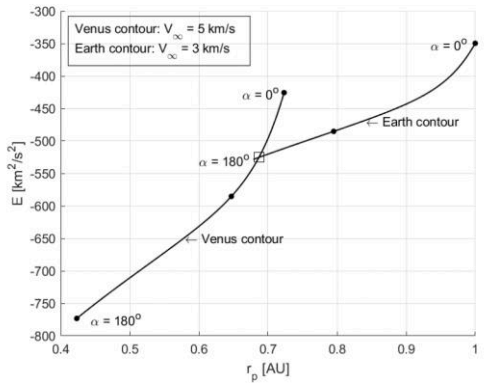


Fig. 2. Infinity velocity contours of 5 km/s and 3 km/s at Venus and Earth, respectively. Tick marks separate flybys with 200 km altitude. The squared mark represents a possible transfer between the two planets

Since the flyby bodies are assumed to be in circular and coplanar orbits, $a_{SC}$ and $e_{SC}$ as obtained from eq. 1 are the only parameters needed to fully describe the orbit of the spacecraft. Equivalently, the orbital energy $E$ and the periapsis $r_p$ entirely define the shape and dimension of the orbit. An $E - r_p$ graph [15] for different planets can be obtained from eq. 1 by fixing a $V_{\infty}$ level and spanning $\alpha$ from $0^{o}$ to $180^{o}$.

Fig. 2 represents the $E - r_p$ Tisserand graph for Venus and Earth with $V_{\infty}$ =5 km/s and $V_{\infty}$ =3 km/s, respectively, namely the coplanar orbit space around the Sun [16]. Tick marks on the contours are separated by flyby at Venus and Earth with $V_{\infty}$=5 km/s and $V_{\infty}$ =3 km/s, respectively, with flyby altitude of 200 km. These can be used to quickly assess the effect of the close passage with the given planet, as they represent the change in the spacecraft orbit effected with the flyby. Moreover, the squared mark at the intersection of the two contours represents a possible transfer orbit between the Earth and Venus. This opportunity only exists from an energy point of view, since Tisserand graphs contain no explicit information regarding the planetary phase and transfer time.

*3.1 Tisserand map exploration*

Exploring a Tisserand map means to evaluate the effect of all possible sequences of planetary swing-bys in the parameters of the Tisserand invariant; i.e. semimajor axis *a*, eccentricity *e*. It is thus possible to enumerate all the planetary sequences which are energetically feasible to reach the desired target orbit. See for example Fig. 3 where swing-by sequences towards Jupiter with a single departure condition at Earth are represented in the $E - r_p$ graph.

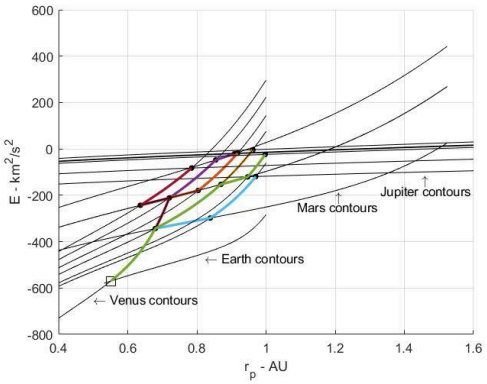


Fig. 3. Some paths towards Jupiter represented on the Tisserand map. Tick marks separate flybys with 200 km altitude. The squared mark represents the departing condition, i.e. a possible transfer between the first two planets

Let us define as a *node* a given position in the Tisserand map (i.e. rp, E), corresponding to a heliocentric orbit. Once a starting node is defined, the second level (i.e. the set of potential reachable new nodes) is constructed by evaluating all the possible planetary swing-bys from the given departing condition.

This is done by considering the intersections between the current node and the orbits of all the planets in the Solar System. If the current node defines an orbit that crosses the orbit of a planet, then a swing-by with this given planet is possible. At each node of the second level, the flybys are evaluated, assuming a minimum allowable swing-by altitude of 200 km, and the resulting orbits are saved. Successive levels are built by checking all the possible flybys from each resulting orbit from the previous level. The search is stopped either when the arrival node or a maximum number of levels (i.e. iterations) is reached.

*3.2 Earth-Jupiter test case: an enumerative exploration*

In order to assess the feasibility of solving an MGA transfer towards Jupiter, one can enumerate all the viable sequences after a given number of iterations. The exploration begins by selecting departing nodes on the map. The starting planet is assumed to be the Earth, with departing infinity velocity contours $V_\infty \in [3,5]\ km/s$ and angles $\alpha \in [-180,180]\ deg$. Nodes on Tisserand map, either along the same infinity velocity contour or at intersection between two different ones, can be used to connect contours on the plot into tours. In this way, it is possible to assess the effectiveness of a given path to reach a specific target orbit on the graph. Tisserand maps exploration is usually performed by discretizing the infinity velocity levels at the celestial bodies passages as well as fixing the flyby altitude to the minimum allowable for the flyby planet (see for example Strange [31], Strange and Longuski [15] or Kloster et al. [16]). Given a current node, the next level is constructed from all nodes that can be reached with a single maximum-deflection flyby. This process is iterated until the path to every node is computed.

A more general approach for automated Tisserand map traversal is introduced here. To truthfully represent possible transfer options between two successive flybys, the $V_\infty$ discretization on the plot is avoided. Since any given point on the Tisserand map represents an orbit around the Sun, one can check the available planets to flyby. Given a departing condition $(V_{\infty,D}, \alpha_D)$, it is possible to evaluate the resulting spacecraft trajectory, and thus to enumerate all the reachable planets. In this way, the first layer is explored. For all the planets identified in the first layer, a maximum deflection flyby is performed, and the resulting orbits are stored. Again, for each of them, one checks all the reachable planets and iterates the procedure until Jupiter is reached. All the routes that have reached the arrival node are saved. This is repeated for different departing combinations of $(V_{\infty,D}, \alpha_D)$. This concludes the enumeration of all the viable sequences towards Jupiter. Since planets phasing is ignored at this stage, these transfers options only exist from the energetic point of view, and one assumes that the flyby planet would be in the proper position to allow the spacecraft to perform the swing-by.

*3.3 Earth-Jupiter MGA Combinatorial and Continuous Optimization*

The previous section completed an enumeration of all the possible sequences towards Jupiter. However, since Tisserand maps contain no explicit information about planets phasing, time of flight requires to be estimated using some relevant approximation and/or specific heuristic. A possible strategy could be to evaluate the transfer time fort the shortest arc connecting the two planets' orbits. However, this usually results in an underestimation of the flight time of more than 30% [15] in the most optimistic cases, as well as it poses strict constraints upon planets positions along their orbits in terms of synodic period. Following Table 2 summarises the sequences obtained. These have been computed by fixing a single departing condition at Earth, i.e. a $(V_{\infty,D}, \alpha_D)$ = (4.9 km/s, 173 deg). In general, one can discretize the departing conditions taking more levels associated to $(V_{\infty,D}, \alpha_D)$. For example, taking 110 departing conditions with equally spaced $V_\infty \in [3,5]\ km/s$ and angles $\alpha \in [-180,180]\ deg$, one can obtain 128 sequences, with a maximum of three flybys.

Table 2. Sequences resulting from the enumerative approach

| Sequences | Time of Flight (years) |
|---|---|
| *EVVEJ | 1.61 |
| EVEEJ | 6.38 |
| EVEMJ | 2.12 |
| EVVVEJ | 4.68 |
| EVVEMJ | 1.54 |
| EVVMEJ | 5.34 |
| EVVMVJ | 4.14 |
| EVEEMJ | 6.43 |
| EVEMEJ | 8.56 |
| EVMEEJ | 3.42 |
| EVMEMJ | 3.54 |

*E = Earth, V = Venus, M = Mars, J = Jupiter

The time of flight along each leg of an MGA transfer can be estimated by considering the spacecraft true anomaly ($\theta_{SC}$) when leaving the first planet of the leg. Fig. 4 illustrates the possible transfers between two circular and coplanar orbits. In Fig. 4, $t_1$ and $t_2$ represent the time from periapsis passage (positive counter clockwise), which are evaluated from Kepler's equations (for elliptical orbits):

$$t_{1,2} = \frac{T}{2\pi}\left(E_{1,2} - e\sin(E_{1,2})\right) \quad (3)$$

Where: $T$ and $e$ are the period and eccentricity of the transfer orbit, respectively, and $E_{1,2}$ is the eccentric anomaly at $t_{1,2}$. Considering only transfers with less than one full revolution (i.e. the first two intersections with the target orbit), eight arcs connect the two orbits. The first four arcs are associated to an upwards transfer (i.e. the spacecraft travels from the innermost to the outermost planet), while the other four are related to a downwards transfer (i.e. the spacecraft travels from the outermost to the innermost planet). Table 3 shows the time of flight computation for each of these permutations.

Table 3. Flight times for possible arcs (only considering first two intersections)

| Spacecraft position | | Upward | Downward |
|---|---|---|---|
| $0 \le \theta_{SC} < \pi$ | *FI | $t_2 - t_1$ | $T - t_2 - t_1$ |
| | SI | $T - t_2 - t_1$ | $T - t_2 + t_1$ |
| $\pi \le \theta_{SC} < 2\pi$ | FI | $t_2 + t_1$ | $t_2 - t_1$ |
| | SI | $T - t_2 + t_1$ | |

* FI = First Intersection, SI = Second Intersection

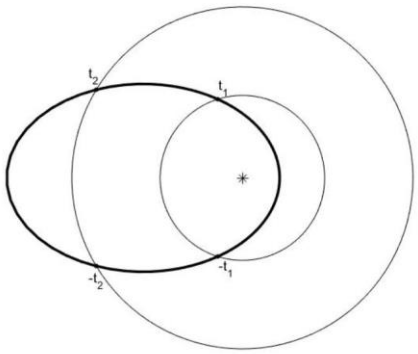


Fig. 4. Possible transfer arcs between two circular and coplanar orbits

If the departing and arrival planets coincide, then there are only two different possibilities associated to $0 \le \theta_{SC} < \pi$ and $\pi \le \theta_{SC} < 2\pi$. If $0 \le \theta_{SC} < \pi$, the spacecraft is at $t_1$ (or equivalently at $t_2$) and the time of flight for the next intersection is $T - 2t_1$ (or equivalently $T - 2t_2$). Otherwise, if $\pi \le \theta_{SC} < 2\pi$, the spacecraft is at $-t_1$ (or equivalently at $-t_2$) and the flight time to the next intersection is $2t_1$ (or equivalently $2t_2$). In both cases, the time of flight to the second intersection is $T$.

## 4. MGA Continuous Optimization

Once all the enumerated routes have been saved, one can classify them as done in Fig. 5. Black squares have been obtained with the enumeration approach and classified as described in Section 3.3; the cost for the Tisserand solutions have been assumed to be the sum of the departing and arrival infinity velocities. These have been obtained with single departing condition, i.e. $V_{\infty,D} = 5\ km/s$ and $\alpha_D = 173\ deg$, towards Jupiter. Red squares are the results of full trajectory optimization: one wants to solve the full problem of finding at least one locally optimal trajectory for the given sequences. Once the planetary sequence is known employing the circular-coplanar model, a full-ephemeris model is used to search for local optimal trajectories.

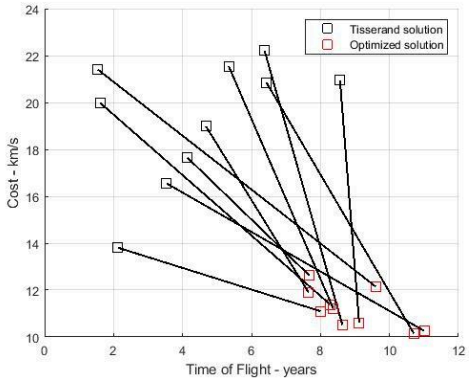


Fig. 5. Solutions for Earth-to-Jupiter transfer as obtained from Tisserand map exploration (black squares) and from optimization (red squares)

Finding optimal trajectories for a given planetary sequence is a complex task on its own. Several methods based on Particle Swarm Optimization (PSO) [32], Genetic Algorithms (GA) [13], Differential Evolution (DE) [26], monotonic basin hopping and ACO [33] are reported in literature.

In the present paper, the sequences identified are optimized with a Particle Swarm Optimization (PSO) [34], [35]. The departing conditions (i.e. departing infinity velocity and $\alpha$ angle) are assumed to be provided by the solutions obtained with Tisserand map exploration. The model used for the optimization is the so-called MGA-1DSM as described by Vasile and De Pascale in [36] where DSMs are assumed on each planet-to-planet trajectory of the path. The objective function to be minimized is the sum of all the DSMs involved in the transfer. Fig. 5 represents solutions as obtained from Tisserand graph exploration (black squares) compared with optimized solution (red squares). As it can be seen, since the required location of the planet is ignored in Tisserand map search, the optimized solutions generally requires higher time of flights. This is because the Tisserand exploration has been performed ignoring the planets positions along their orbits. In this way, these solutions do not provide information on the shape of the trajectory, but only the planetary sequence is known.

## 5. Solving the phasing problem

The previous section showed that ignoring planets phasing when looking for optimal trajectories leads to infeasible paths. In other words, the optimized solutions only share the same planetary sequence with Tisserand map, meaning that no information about the shape of the trajectory nor a proper time of flight estimation is provided from Tisserand map exploration. In order to answer this issue, solving the phasing problem becomes crucial to obtain better representation of the final trajectory directly from Tisserand map exploration.

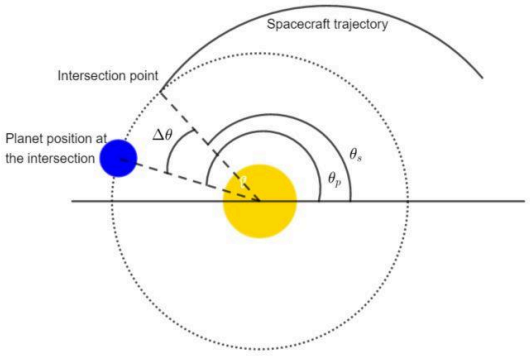


Fig. 6. Illustration of the phasing problem

Performing a flyby manoeuvre implies the matching between the spacecraft position and that of the planet. From Fig. 3, if the spacecraft leaves the inner planet at $t_1$ to reach the outer one, at the first intersection time $t_{int} = t_2 - t_1$ the planet true anomaly $\theta_p$ would be in general different from that of the spacecraft $\theta_s$ (see also Fig. 6). The anomaly $\theta_s$ depends upon the orbit resulting after the last planetary encounter, i.e. the flyby radius $r_p$ of the previous swing-by planet or the infinity velocity at the departure velocity vector $v_0$ (if the first leg is considered). Therefore, $\Delta\theta = \theta_p - \theta_s$ can be expressed as function of the variable $x$, such that $x = r_p$ if flyby, or $x = v_0$ if launch. First four intersections are considered each time the spacecraft can perform a flyby with a given planet. From Table 3, if more than two intersections are considered, one simply applies $tof = tof_1 + NT$, if the $2N+1$ intersection is considered, while $tof = tof_2 + (N+1)T$, if the $2N+2$ intersection is considered. As described in Section 3.3, $tof_1$ and $tof_2$ are computed based upon the transfer option (upwards/downwards).

In this paper, we are not considering $N > 1$ as in most practical missions transfer time is limited, and larger N would imply longer transfers. It is worth noticing that considering $N \geq 1$ for a same-planet-to-same-planet transfer corresponds to look for resonances along the given infinity velocity contour. The solution of the phasing problem is $x^*$ such that $\Delta\theta(x^*) = \theta_p(x^*) - \theta_s(x^*) = 0$. The Brent's method is employed to find $x^*$. Intervals for the bisection method need to be provided to initialize the method and are specified case by case.

### *5.1 Complete Ballistic Search*

This section describes the automatic exploration of the Tisserand graph with proper time of flight estimation as highlighted in previous section. The search starts by selecting a departing condition in terms of $(V_\infty, \alpha)$. If the resulting orbit crosses one or more planets orbits, then a possible flyby option with the given planet exists from the energetic point of view (first four intersections with the target planet are considered). The time of flight is computed as described in Section 3.3This provides the first two planets of the sequence and the state at each of them. For all the possible options identified, a maximum deflection flyby is computed (both in-front and behind the planet), and the resulting orbit is saved. Again, if this crosses one or more planets orbits, a possible transfer exists (from the energetic point of view). This would be a real trajectory only if $\Delta\theta(x) = f(r_p) = 0$ (first four intersections are considered for both in-front and behind passages of the current flyby planet). Only the options for which at least a solution to $\Delta\theta(x) = f(r_p) = 0$ exists are stored. All the other options are discarded. This provides the next planet to flyby. The procedure is repeated until a stopping condition is reached. This automatically provides all the possible flyby options for the given combination of departing date and $(V_\infty, \alpha)$. The purely ballistic MGA combinatorial problem is thus solved (no DSMs are considered at this stage). The time of flight between two successive planets is computed as described in Section 3.3 once the solution of $\Delta\theta = f(h_p) = 0$ is available.

## 6. Results

In this section, results for the Earth-Jupiter transfer case are shown and compared to existing literature. From Fig. 3, there exist several flyby options to reach high energy orbits around the Sun, exploiting close passages with Venus, Earth and Mars. Combinations of successive flybys between these planets are useful to increase spacecraft perihelion, as well as maintaining low propellant consumption when reaching Jupiter (i.e. low infinity velocities at the arrival correspond to low $\Delta v$ when considering Jupiter orbit insertion). However, these options exist only from the energetic point of view.

The actual trajectory is found by solving the phasing problem as described in Section 5.1. The aim is to show that the Tisserand exploration with modified time of flight computation already provides good approximation of the full trajectory.

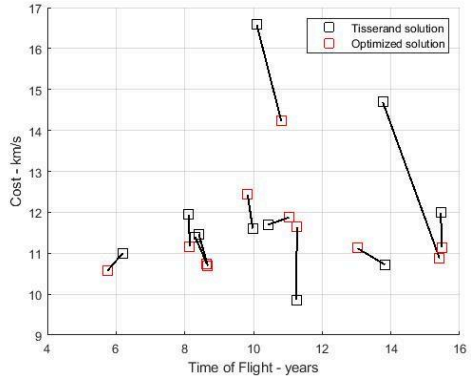


Fig. 7. Solutions for Earth-to-Jupiter transfer as obtained from modified Tisserand map exploration (black squares) and from optimization (red squares)

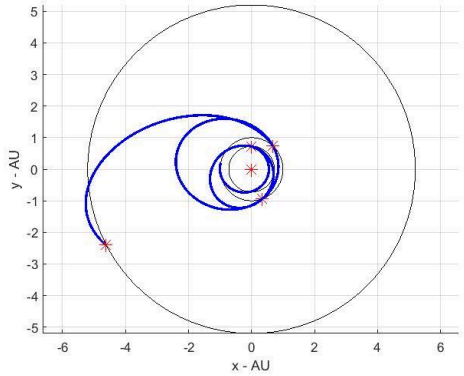


Fig. 8. Earth-Venus-Earth-Earth-GA path towards Jupiter (Galileo-like trajectory) as obtained from modified Tisserand map exploration

The design parameters and their upper and lower bounds are reported in Table 4. Minimum and maximum flyby altitudes are assumed to be 200 km and 35000 km over the planet surface, respectively.

Fig. 7 provides representation of the sequences obtained with the complete ballistic search as described in Section 5 and Section 5.1. The solutions obtained share the same planetary sequence as in Table 2, but they have been obtained by solving the phasing problem at each iteration of the procedure in Section 5.1. As it can be seen, solutions obtained with Tisserand exploration already provide good representation of the final set of trajectories. In this way, not only the planetary sequence is known, but also the trajectory shape, namely cost and time of flight, is provided.

Fig. 8 and Fig. 9 show two examples of transfer towards Jupiter exploiting flybys with Earth, Venus and Mars resulting from modified Tisserand map exploration. In particular, the classic Earth-Venus-Earth-Earth-GA (the same path used for Galileo [1]) and Earth-Venus-Earth-Mars-Earth-GA (a JUICE-like trajectory [24]) as obtained from the circular-coplanar model are reported.

Table 4. Lower and upper bounds for parameters involved in full trajectory optimization

| Parameter | Description | Lower Bound | Upper Bound |
|---|---|---|---|
| $TOF_i$ (days) | Time of flight for the leg $i$ | -15% of Tisserand solution | +15% of Tisserand solution |
| $\alpha_i$ | Fraction of $TOF_i$ at which a DSM occurs | 0 | 1 |
| $\gamma_{i+1}$ (deg) | Hyperbola plane inclination at the planet $i+1$ | -180 | 180 |
| $h_{p,i+1}$ (km) | Flyby altitude at the planet $i+1$ | *Min. flyby altitude at the planet | *Max. flyby altitude at the planet |
| $t_0$ (MJD2000) | Departing date | -10% of Tisserand solution | +10% of Tisserand solution |
| $V_{\infty,D}$ (km/s) | Departing infinity velocity | -5% of Tisserand solution | +5% of Tisserand solution |
| $\alpha_D$ (deg) | Departing angle | -5% of Tisserand solution | +5% of Tisserand solution |

*Min. = Minimum, Max. = Maximum

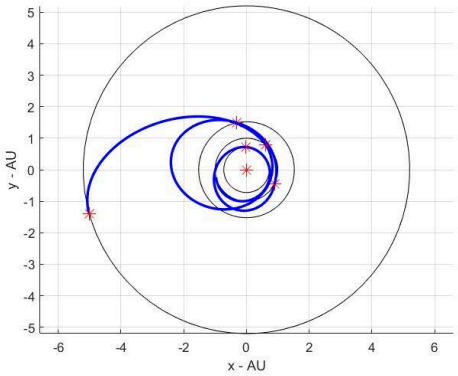


Fig. 9. Earth-Venus-Earth-Mars-Earth-GA path towards Jupiter (JUICE-like trajectory) as obtained from modified Tisserand map exploration

In Fig. 10 and Fig 11, the same paths have been optimized once the trajectory from modified Tisserand exploration is provided. Both transfers are consistent with literature findings (see Petropoulos et al. [25] and Ecale et al. [24]). One can appreciate that the trajectory resulting from Tisserand map exploration with complete ballistic search and modified time of flight computation

provides a good guess of the full trajectory (in both cases the total DSMs cost is less than 500 m/s), both in terms of time of flight and flyby altitudes.

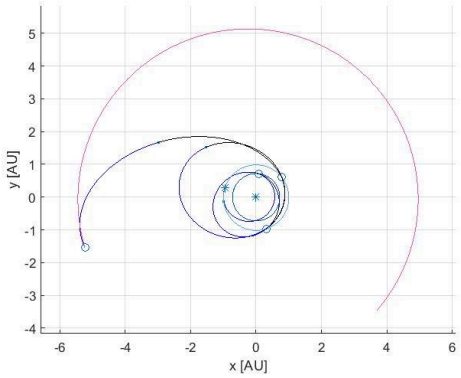


Fig. 10. Earth-Venus-Earth-Earth-GA path towards Jupiter (Galileo-like trajectory) as obtained from full optimization once the Tisserand solution is provided

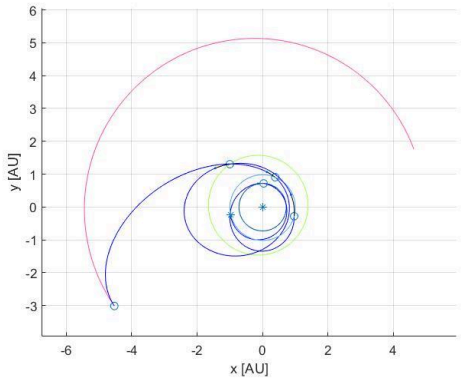


Fig. 11. Earth-Venus-Earth-Mars-Earth-GA path towards Jupiter (JUICE-like trajectory) as obtained from full optimization once the Tisserand solution is provided

## 7. Conclusions

The present paper has presented a novel approach to Tisserand map-based sequence generation, accounting for planets positions along their orbits, thus solving the phasing problem. This is because current Tisserand map sequence generator approaches seem to lack in providing information about trajectory shape, namely planetary phasing and timing. The proposed modified Tisserand map-based approach allows to automatically generate planetary sequence with enough information regarding trajectory shape, with focus on mission duration. The modified Tisserand map approach has been tested for the well-known Earth-to-Jupiter transfer case, and all the trajectories have been re-optimized through complete MGA transfers as sequences of flybys and Deep Space Manoeuvres (DSMs), validating the accuracy of Tisserand-based first-guess solutions. The presented work has shown promising results; however, evolution and refinement are needed. Future research will also focus on implementing small DSMs during the modified Tisserand map search.


## Acknowledgements

This work was supported by Airbus Defence and Space through the Cranfield University Industrial Partnership Framework (MITnTargets: Mixed-Integer Trajectory Design for Large Number of Targets).


## References


[1] L. A. D'Amario, D. V Byrnes, J. R. Johannesen, and B. G. Nolan, "Galileo 1989 VEEGA trajectory design," *J. Astronaut. Sci.*, vol. 37, pp. 281–306, 1989.

[2] F. Peralta and S. Flanagan, "Cassini interplanetary trajectory design," *Control Eng. Pract.*, vol. 3, no. 11, pp. 1603–1610, 1995.

[3] N. J. Fox *et al.*, "The solar probe plus mission: humanity's first visit to our star," *Space Sci. Rev.*, vol. 204, no. 1–4, pp. 7–48, 2016.

[4] J. M. Sanchez Perez, W. Martens, and G. I. Varga, "Solar orbiter 2020 february mission profile," in *Advances in the Astronautical Sciences*, 2018, vol. 167, pp. 1395–1410.

[5] M. Schlueter, S. O. Erb, M. Gerdts, S. Kemble, and J.-J. Rückmann, "MIDACO on MINLP space applications," *Adv. Sp. Res.*, vol. 51, no. 7, pp. 1116–1131, 2013.

[6] I. M. Ross and C. N. D'Souza, "Hybrid optimal control framework for mission planning," *J. Guid. Control. Dyn.*, vol. 28, no. 4, pp. 686–697, 2005.

[7] C. M. Chilan and B. A. Conway, "A space mission automaton using hybrid optimal control," in *17th Annual Space Flight Mechanics Meeting*, 2007, pp. 259–276.

[8] B. J. Wall and B. A. Conway, "Genetic algorithms applied to the solution of hybrid optimal control problems in astrodynamics," *J. Glob. Optim.*, vol. 44, no. 4, p. 493, 2009.

[9] J. A. Englander, B. A. Conway, and T. Williams, "Automated mission planning via evolutionary algorithms," *J. Guid. Control. Dyn.*, vol. 35, no. 6, pp. 1878–1887, 2012.

[10] J. Englander, B. Conway, and T. Williams, "Automated interplanetary trajectory planning," in *AIAA/AAS Astrodynamics Specialist Conference*, 2012, p. 4517.

[11] M. Ceriotti and M. Vasile, "Automated multigravity assist trajectory planning with a modified ant colony algorithm," *J. Aerosp. Comput. Information, Commun.*, vol. 7, no. 9, pp. 261–293, 2010.

[12] M. Ceriotti and M. Vasile, "MGA trajectory planning with an ACO-inspired algorithm," *Acta Astronaut.*, vol. 67, no. 9–10, pp. 1202–

1217, 2010.
[13] A. Gad and O. Abdelkhalik, “Hidden genes genetic algorithm for multi-gravity-assist trajectories optimization,” *J. Spacecr. Rockets*, vol. 48, no. 4, pp. 629–641, 2011.
[14] O. Abdelkhalik and A. Gad, “Dynamic-size multiple populations genetic algorithm for multigravity-assist trajectory optimization,” *J. Guid. Control. Dyn.*, vol. 35, no. 2, pp. 520–529, 2012.
[15] N. J. Strange and J. M. Longuski, “Graphical method for gravity-assist trajectory design,” *J. Spacecr. Rockets*, vol. 39, no. 1, pp. 9–16, 2002.
[16] K. W. Kloster, A. E. Petropoulos, and J. M. Longuski, “Europa Orbiter tour design with Io gravity assists,” *Acta Astronaut.*, vol. 68, no. 7–8, pp. 931–946, 2011.
[17] G. Colasurdo, A. Zavoli, A. Longo, L. Casalino, and F. Simeoni, “Tour of Jupiter Galilean moons: Winning solution of GTOC6,” *Acta Astronaut.*, vol. 102, pp. 190–199, 2014.
[18] Y. Chen, H. Baoyin, and J. Li, “Accessibility of main-belt asteroids via gravity assists,” *J. Guid. Control. Dyn.*, vol. 37, no. 2, pp. 623–632, 2014.
[19] P. Sun, H. Yang, and S. Li, “Accessibility of near-Earth asteroids and main-belt asteroids in a gravity-assisted multi-target mission,” *Planet. Space Sci.*, vol. 182, p. 104851, 2020.
[20] A. Törn, M. M. Ali, and S. Viitanen, “Stochastic global optimization: Problem classes and solution techniques,” *J. Glob. Optim.*, vol. 14, no. 4, pp. 437–447, 1999.
[21] D. Izzo, “1st ACT global trajectory optimisation competition: Problem description and summary of the results,” *Acta Astronaut.*, vol. 61, no. 9, pp. 731–734, 2007.
[22] M. Meltzer, “Mission to Jupiter: a history of the Galileo project,” *STIN*, vol. 7, p. 13975, 2007.
[23] O. Grasset *et al.*, “JUpiter ICy moons Explorer (JUICE): An ESA mission to orbit Ganymede and to characterise the Jupiter system,” *Planet. Space Sci.*, vol. 78, pp. 1–21, 2013.
[24] E. Ecale, F. Torelli, and I. Tanco, “JUICE interplanetary operations design: drivers and challenges,” in *2018 SpaceOps Conference*, 2018, p. 2493.
[25] A. E. Petropoulos, J. M. Longuski, and E. P. Bonfiglio, “Trajectories to Jupiter via gravity assists from Venus, Earth, and Mars,” *J. Spacecr. Rockets*, vol. 37, no. 6, pp. 776–783, 2000.
[26] A. D. Olds, C. A. Kluever, and M. L. Cupples, “Interplanetary mission design using differential evolution,” *J. Spacecr. Rockets*, vol. 44, no. 5, pp. 1060–1070, 2007.
[27] D. A. Vallado, *Fundamentals of astrodynamics and applications*, vol. 12. Springer Science & Business Media, 2001.
[28] R. H. Battin, *An Introduction to the Mathematics and Methods of Astrodynamics, revised edition*. American Institute of Aeronautics and Astronautics, 1999.
[29] F. Tisserand, *Traité de mécanique céleste*. Gauthier-Villars, 1891.
[30] J. Miller and C. Weeks, “Application of Tisserand’s criterion to the design of gravity assist trajectories,” in *AIAA/AAS Astrodynamics Specialist Conference and Exhibit*, 2002, p. 4717.
[31] N. J. Strange, “Analytical methods for gravity-assist tour design,” 2016.
[32] M. Pontani and B. A. Conway, “Particle swarm optimization applied to space trajectories,” *J. Guid. Control. Dyn.*, vol. 33, no. 5, pp. 1429–1441, 2010.
[33] M. Vasile, E. Minisci, and M. Locatelli, “Analysis of some global optimization algorithms for space trajectory design,” *J. Spacecr. Rockets*, vol. 47, no. 2, pp. 334–344, 2010.
[34] R. Eberhart and J. Kennedy, “A new optimizer using particle swarm theory,” in *MHS’95. Proceedings of the Sixth International Symposium on Micro Machine and Human Science*, 1995, pp. 39–43.
[35] J. Kennedy and R. Eberhart, “Particle swarm optimization,” in *Proceedings of ICNN’95-International Conference on Neural Networks*, 1995, vol. 4, pp. 1942–1948.
[36] M. Vasile and P. De Pascale, “Preliminary design of multiple gravity-assist trajectories,” *J. Spacecr. Rockets*, vol. 43, no. 4, pp. 794–805, 2006.

https://dspace.org/

# Modified tisserand map exploration for preliminary multiple gravity assist trajectory design

**Bellome, Andrea; Cuartielles, Joan-Pau Sanchez; Felicetti, Leonard; Kemble, Stephen**

**2020-10-14**
IAFASTRO
https://www.iafastro.org/events/iac/iac-2020/
Bellome A, Sanchez Cuartielles J-P, Felicetti L. et al., (2020) Modified tisserand map exploration for preliminary multiple gravity assist trajectory design. In: 71st International Astronautical Congress - the Cyberspace Edition, 12-14 October 2020,Online

Downloaded from a DSpace repository. https://dspace.org/